

Accuracy of Swan–Ganz catheterization-based assessment of right ventricular function: Validation study using high-fidelity micromanometry-derived values as reference

Hideki Shima¹ | Toshitaka Nakaya¹ | Ichizo Tsujino^{1,2}  | Junichi Nakamura¹ | Ayako Sugimoto¹ | Takahiro Sato^{1,2} | Taku Watanabe¹ | Hiroshi Ohira¹ | Masaru Suzuki¹ | Masaru Kato³ | Isao Yokota⁴ | Satoshi Konno¹

¹Department of Respiratory Medicine, Faculty of Medicine, Hokkaido University, Sapporo, Japan

²Division of Respiratory and Cardiovascular Innovative Research, Faculty of Medicine, Hokkaido University, Sapporo, Japan

³Department of Rheumatology, Endocrinology and Nephrology, Faculty of Medicine and Graduate School of Medicine, Hokkaido University, Sapporo, Japan

⁴Department of Biostatistics, Graduate School of Medicine, Hokkaido University, Sapporo, Japan

Correspondence

Ichizo Tsujino, Division of Respiratory and Cardiovascular Innovative Research, Faculty of Medicine, Hokkaido University, North 14, West 5, Kita-ku, Sapporo 060-8648, Japan.

Email: itsuji@med.hokudai.ac.jp

Funding information

None

Abstract

Right ventricular (RV) function critically affects the outcomes of patients with pulmonary hypertension (PH). Pressure wave analysis using Swan–Ganz catheterization (SG-cath) allows for the calculation of indices of RV function. However, the accuracy of these indices has not been validated. In the present study, we calculated indices of systolic and diastolic RV functions using SG-cath-derived pressure recordings in patients with suspected or confirmed PH. We analyzed and validated the accuracies of three RV indices having proven prognostic values, that is, end-systolic elastance (Ees)/arterial elastance (Ea), β (stiffness constant), and end-diastolic elastance (Eed), using high-fidelity micromanometry-derived data as reference. We analyzed 73 participants who underwent SG-cath for the diagnosis or evaluation of PH. In this study, Ees/Ea was calculated via the single-beat pressure method using $[1.65 \times (\text{mean pulmonary arterial pressure}) - 7.79]$ as end-systolic pressure. SG-cath-derived Ees/Ea, β , and Eed were 0.89 ± 0.69 (mean \pm standard deviation), 0.027 ± 0.002 , and 0.16 ± 0.02 mmHg/ml, respectively. The mean differences (limits of agreement) between SG-cath and micromanometry-derived data were 0.13 (0.99, -0.72), 0.002 (0.020, -0.013), and 0.04 (0.20, -0.12) for Ees/Ea, β , and Eed, respectively. The intraclass correlation coefficients of the indices derived from the two catheterizations were 0.76, 0.71, and 0.57 for Ees/Ea, β , and Eed, respectively. In patients with confirmed or suspected PH, SG-cath-derived RV indices, especially Ees/Ea and β , exhibited a good correlation with micromanometry-derived reference values.

KEYWORDS

high-fidelity micromanometry, pulmonary hypertension, right ventricular function, Swan–Ganz catheterization

This is an open access article under the terms of the Creative Commons Attribution-NonCommercial License, which permits use, distribution and reproduction in any medium, provided the original work is properly cited and is not used for commercial purposes.

© 2022 The Authors. *Pulmonary Circulation* published by John Wiley & Sons Ltd on behalf of Pulmonary Vascular Research Institute.

INTRODUCTION

The right ventricular (RV) function is critically important in the management of pulmonary hypertension (PH).^{1,2} A variety of indices are used to assess RV function, such as cardiac output, tricuspid annular plane systolic excursion, and RV ejection fraction (EF).³ However, these indices are subject to change under different pre- and after-loads and, thus do not reflect the “intrinsic” RV function.

The intrinsic RV function comprises contractility and diastolic function (relaxation and compliance).^{1,4} Gold standard indices for these functions are end-systolic elastance (Ees) for contractility, tau for relaxation, β and end-diastolic elastance (Eed) for compliance/elastance. Another emerging element of RV function is RV-pulmonary arterial (PA) coupling, represented as Ees/[arterial elastance (Ea)]. Previous studies, including ours, have reported the promising prognostic roles of these indices.^{5–8}

In most previous studies, these RV indices were calculated using Swan–Ganz catheterization (SG-cath)-derived pressure and its derivatives, including isovolumic pressure (Piso). However, a Swan–Ganz catheter is a compliant water-filled catheter that has innate inaccuracies, such as bending and distortion, pressure blurring due to air bubbles, and attenuation of high frequencies.^{9,10} Consequently, some RV indices, calculated using SG-cath, may not be free from catheter-related errors. In fact, it is commonly observed that pressure waves recorded via SG-cath show fluctuations or noises that may impede the reliability of the obtained pressure and its derivatives.

In Japan, a thin modified pressure catheter used for high-fidelity micromanometry (Pressure-cath) became available in 2017. This enables accurate RV pressure (RVP) measurements with less invasiveness and a shorter examination time than its previous model. This modified pressure catheter enables successive measurements of RVP using both SG- and Pressure-cath with a clinically acceptable examination time and invasiveness. Notably, the gold standard method for calculating indices of RV function requires a simultaneous application of pressure and conductance catheterizations, which enable drawings of multiple pressure-volume loops.¹¹ However, Pressure-cath is a reliable modality that enables more accurate RVP recording and calculations of RV indices, at least, compared to SG-cath.

In this study, we aimed to validate the accuracy of SG-cath-derived indices of RV function. Specifically, we aimed to determine whether RV indices having prognostic values, such as Ees/Ea and β , were significantly correlated with the corresponding Pressure-cath-derived

values, and whether the correlation coefficients were acceptably high.

METHODS

Study participants

We collected data from a series of patients with suspected or confirmed PH who underwent right heart catheterization at our hospital between May 2020 and December 2021. In patients with confirmed PH, the diagnosis, classification, and management of PH were performed according to the guidelines for PH published in 2015.¹² Patients also underwent cardiac magnetic resonance imaging (CMRI) when possible.

This study was approved by the institutional review board of our institution. Owing to the retrospective nature of the study, informed consent was obtained on an opt-out basis, via our institution website. Patient identity was concealed, and all data were compiled according to the requirements of the Japanese Ministry of Health, Labor, and Welfare. Moreover, this study was conducted in accordance with the 1964 Declaration of Helsinki and its later amendments.

Right heart catheterization

Assessment of pulmonary hemodynamics via SG-cath

Participants underwent SG-cath according to the methods recommended in the guidelines for PH.¹² Briefly, with the patient in the supine position, a 6-French sheath was placed through the right internal jugular or femoral vein, and a Swan–Ganz catheter was inserted and advanced into the pulmonary artery. The catheter was connected to a polygraph (RMC-4000; Nihon Kohden Corporation). PA pressure, PA wedge pressure, CO, RVP, and right atrial pressure were recorded. The RV end-diastolic pressure (RVEDP) was measured immediately before a rapid upstroke in RVP.¹³ The zero level was determined at the mid-level of the chest wall.¹⁴ All pressure measurements were performed at the end of normal expiration (without breath holding), while additional diastolic RVP measurements of at least five cardiac cycles were performed with breath holding at the end of normal expiration. These recommendations related to breathing were in accordance with the guidelines of PH management.¹² Cardiac output was measured using the thermodilution method, and the mean of at least three measurements was used as the representative value.

Measurement of RVP using a high-fidelity micromanometer

Immediately after SG-cath, the Swan–Ganz catheter was removed and a 5-F or 6-F guiding catheter (Mach 1™ Coronary Guide Catheter, Boston Scientific) was inserted and advanced to the right ventricle. Subsequently, a pressure catheter (Micro-Cath™ pressure catheter, Millar Co., Ltd.) was inserted through the guiding catheter into the right ventricle. The pressure catheter was connected to an AV converter (PowerLab®, ADInstruments), and then to a personal computer wherein a dedicated software (LabChart Pro®, ADInstruments) was installed to allow for real-time pressure recording at 1000 Hz. The zero level was determined before the pressure catheter was inserted into the guiding catheter, by placing the tip of the catheter immediately below the surface of warm water in a cup. RVP was recorded at natural end-expiration. At least five consecutive RVP curves were recorded and analyzed. These processes of Pressure-cath were completed within approximately 15 min, without any significant changes in circulatory and respiratory conditions.

Assessment of RV morphology using CMRI

CMRI was performed using a 1.5-T Achieva scanner (Philips Medical Systems) with a five-channel coil and master gradients (maximum gradient amplitude, 33 mT/m; maximum slew rate, 100 mT/m/ms). Furthermore, CMRI was performed within 14 days from the date of right heart catheterization, during which there were no significant changes in either hemodynamic status or PH treatment. Image acquisition and analysis were performed using a previously described protocol, with high intra- and interobserver reproducibilities.¹⁵ Briefly, 12 axial slices were acquired using a steady-state free-precession pulse sequence (repetition time, 2.8 ms; echo time, 1.4 ms; flip angle, 60; acquisition matrix, 192 × 256; field of view, 380 ms; slice thickness, 10 mm; 0 mm inter-slice gap; and 20 phases/cardiac cycle). Images were analyzed using commercially available analysis software (Extended MR Work Space ver. 2.6.3; Philips Medical Systems). In the axial datasets, the endocardial contours of the right ventricle were manually traced, and the RV and left ventricular end-diastolic volume (EDV) and end-systolic volume (ESV) were computed. RV and left ventricular stroke volume (SV) and EF were calculated as $SV = EDV - ESV$ and $EF = SV/EDV \times 100\%$, respectively.

Assessment of RV function

Analysis of SG-cath- and Pressure-cath-derived RVP indices

RVP data recorded via SG- and Pressure-cath were analyzed offline using LabChart Pro®.

Five stable, consecutive RVP curves were selected, and the mean of five maximum RVPs (systolic RVP [SRVP]), minimum RVP (RVP-min), RVEDP, maximum dp/dt (dp/dt-max), minimum dp/dt (dp/dt-min), tau, and Piso were calculated. RVEDP was determined using a dedicated program for RVP analysis bundled in LabChart Pro®. Piso calculation was performed using LabChart Pro® based on the single-beat method reported by Bellofiore et al.¹⁶ In this method, sine-wave curves were fitted (curve fitting) to the early systolic and early diastolic portions of the RVP curve, and the peak pressure value of the sine-wave for one cardiac cycle was read as Piso.¹⁷ The mean of five consecutive Piso values was used as the representative value. Tau was calculated using the Weiss and Logistic methods.^{18,19}

Calculations of Ees, Ees/Ea, β , and Eed

Ees was calculated using the following formula (single-beat method)^{16,20}:

$$Ees = (Piso - Pes) / RVS SV \quad (1)$$

Here, Pes represents end-systolic pressure. The gold standard method to determine Pes is the multiple pressure-volume (PV)-loop analysis (multiple beat method) in which conductance and pressure catheterization are simultaneously applied.¹¹ However, in the present study, we did not conduct multiple PV-loop analysis; contrariwise, we used three surrogate parameters for Pes, that is, mean PA pressure (MPAP), calculated pressure using MPAP (MPAPcalc, calculated as $1.65 \times MPAP - 7.79$), and SRVP, as reported in previous studies.^{6,8,17,20–24} When MPAP was used for Pes, Ees was represented as Ees (MPAP); when MPAPcalc was used for Pes, Ees was represented as Ees (MPAPcalc); and when SRVP was used for Pes, Ees was represented as Ees (SRVP). SG-cath-derived MPAP was used in the calculations of Ees (MPAP) and Ees (MPAPcalc). Alternatively, SG-cath- and Pressure-cath-derived SRVP were used for the calculations of SG-cath- and Pressure-cath-derived Ees/Ea (SRVP), respectively. RVS SV represents the RV SV calculated from CMRI.

Ees/Ea is the ratio of Ees to Ea, where Ea is estimated as the ratio of Pes to CMRI-derived RVS SV.²⁰

$$Ea = Pes/RVSV: \quad (2)$$

Ees/Ea was then calculated from Equations (1) and (2).

$$Ees/Ea = P_{iso}/Pes-1: \quad (3)$$

This method of Ees/Ea calculation is called the “pressure method” because only pressure data are used for calculating Ees/Ea. Here, Ees/Ea ratios calculated using MPAP, MPAPcalc, and SRVP as Pes were represented as Ees/Ea (MPAP), Ees/Ea (MPAPcalc), and Ees/Ea (SRVP), respectively.

Another method for calculating Ees/Ea is the “volume method,” in which only volume data are used.²⁰ In this method, Ees is represented as Pes/RVESV. Thus, Ees/Ea can be calculated by $[Pes/RVESV]/[Pes/RVSV]$, which leads to the following equation.

$$Ees/Ea(Vol) = RVSV /RVESV \quad (4)$$

β was calculated as a solution of the following two simultaneous equations, as reported by Rain et al.⁷

$$RVP = \alpha(e^{RVV \cdot \beta} - 1): \quad (5)$$

Here, RVV represents RV volume, and the following three points of pressure and volume were used to calculate α and β : (RVP, RVV); (0, 0), (RVP-min, RVESV), and (RVEDP, RVEDV). RVP-min was normalized at 1 mmHg and, only in this calculation, RVEDP was modified by a formula of $[1 + (RVEDP - RVP\text{-min})]$, to avoid measurement errors.⁷

Eed was calculated as the slope of the diastolic pressure-volume relationship at end-diastole, using the formula previously described by Trip et al.⁸

$$Eed = \alpha \cdot \beta \cdot e^{RVEDV \cdot \beta}: \quad (6)$$

All RV indices were calculated using both SG- and Pressure-cath.

Data analysis

Categorical variables are expressed as absolute numbers (percentages) and continuous variables as means \pm standard deviations (SDs) or medians (interquartile ranges), as appropriate. Using Bland-Altman analysis and intraclass correlation coefficients (ICCs), we evaluated SG-cath-derived RVP and RV indices (dp/dt-max, dp/dt-min, tau [Weiss], tau [Logistic], Ees [MPAP], Ees [MPAPcalc], Ees [SRVP], Ees/Ea [MPAP], Ees/Ea [MPAPcalc], Ees/Ea [SRVP], β , and Eed) using the

corresponding Pressure-cath-derived variables as reference. The 95% limits of agreement were calculated by mean $\pm 1.96 \times$ SD. A high ICC ranging between 0 and 1 indicated high similarity between SG- and Pressure-cath-derived data.²⁵ The sample size was not calculated and all consecutive participants who were eligible for the present study during the study period were included. JMP Pro version 14 (SAS Institute Inc.) was used for statistical analyses.

RESULTS

Table 1 shows the demographic characteristics of the 73 participants, 57 of whom were diagnosed with PH. The other 16 individuals underwent SG-cath with a suspicion of PH; however, they did not fulfill the criteria for PH, as their MPAP and pulmonary vascular resistance were ≤ 20 mmHg and ≤ 3 Wood units, respectively, and so were analyzed as controls.

Table 2 shows the results of CMRI and SG-cath of the 73 participants. CMRI was performed in 50 of the 73 patients.

Figure 1 shows representative images of RVP waves recorded via SG- and Pressure-cath in a 43-year-old woman with heritable PA hypertension. Notably, SG-cath-derived RVPs showed fluctuations or notches near end-diastole (bottom arrow) and after the steep increase in the systolic phase (top arrow; Figure 1a), whereas Pressure-cath-derived RVPs showed no or slight fluctuations/notches (Figure 1b). In addition, SG-cath-derived RVP and calculated indices of RV function, including Ees/Ea (MPAP), Ees/Ea (MPAPcalc), dp/dt-max, β , and Eed, were higher than those obtained via Pressure-cath.

Table 3 shows comparisons of pulmonary hemodynamic parameters between SG- and Pressure-cath. Bland-Altman analysis showed no systematic trends in the values of the parameters. All limits of agreement included 0, and there were no significant differences between SG-cath- and Pressure-cath-derived values (Figure 2). ICCs between SG- and Pressure-cath-derived data are shown in Table 3. The time difference between SG- and Pressure-cath RVP recordings was 12 (11, 16) min.

Table 4 shows the SG- and Pressure-cath-derived data in controls and in patients with PH.

DISCUSSION

The present study is the first to validate the accuracy of SG-cath-derived indices of RV function, using Pressure-cath-derived data as reference, in patients with

TABLE 1 Characteristics of the study population

| | Total subjects (<i>n</i> = 73) | Pulmonary hypertension (<i>n</i> = 57) | Controls (<i>n</i> = 16) |
|--|---------------------------------|---|---------------------------|
| Age (years) | 58 ± 16 | 56 ± 17 | 62 ± 10 |
| Sex (female/male) | 49/24 | 35/22 | 14/2 |
| Body mass index (kg/m ²) | 23 ± 5 | 23 ± 5 | 22 ± 6 |
| Pulmonary hypertension group (1/2/3/4/5) | | 33/0/11/12/1 | NA |
| WHO functional class (I/II/III/IV) | | 12/15/28/2 | NA |
| Use of pulmonary vasodilator(s) | | | NA |
| None | | 17 | |
| Single drug | | 10 | |
| Double combination | | 18 | |
| Triple combination | | 12 | |

Abbreviations: NA, not applicable; WHO, World Health Organization.

TABLE 2 Results of Swan–Ganz catheterization and cardiac magnetic resonance imaging

| Swan–Ganz catheterization | | | |
|------------------------------------|----------------------|------------------------------|----------------|
| <i>n</i> | Total subjects 73 | Pulmonary hypertension 57 | Controls 16 |
| PAWP (mmHg) | 7.6 ± 2.7 | 8.0 ± 2.7 | 6.3 ± 2.4 |
| MPAP (mmHg) | 28.9 ± 11.2 | 32.5 ± 10.0* | 16.1 ± 3.9 |
| RVEDP (mmHg) | 7.1 ± 3.0 | 7.9 ± 2.7* | 4.4 ± 2.6 |
| RAP (mmHg) | 3.8 ± 2.4 | 4.2 ± 2.4 | 2.3 ± 2.0 |
| CO (L/min) | 4.5 ± 1.0 | 4.5 ± 1.1 | 4.5 ± 1.0 |
| CI (L/min/m ²) | 2.8 ± 0.6 | 2.8 ± 0.6 | 2.9 ± 0.5 |
| PVR (Wood unit) | 5.2 ± 3.5 | 6.0 ± 3.6* | 2.2 ± 0.9 |
| Cardiac magnetic resonance imaging | | | |
| <i>n</i> | Total subjects 50 | Pulmonary hypertension 40 | Controls 10 |
| RV end-diastolic volume (ml) | 167.8 ± 90.4 | 182.5 ± 95.0* | 109.0 ± 23.0 |
| RV end-systolic volume (ml) | 110.6 ± 84.3 | 125.1 ± 88.3* | 52.9 ± 15.9 |
| RV stroke volume (ml) | 56.0 ± 19.4 | 56.0 ± 21.2 | 56.1 ± 9.9 |
| RV ejection fraction (%) | 39.2 ± 13.3 | 35.8 ± 12.4* | 53.0 ± 6.5 |
| Ees/Ea (Vol) | 0.72 ± 0.39 | 0.61 ± 0.32* | 1.14 ± 0.40 |

Note: Data are presented as mean ± standard deviation (SD).

Abbreviations: CI, cardiac index; CO, cardiac output; Ees/Ea (Vol), Ees/Ea calculated with the volume method ([RV stroke volume]/[RV end-systolic volume]); MPAP, mean pulmonary arterial pressure; PAWP, pulmonary arterial wedge pressure; PVR, pulmonary vascular resistance; RAP, right atrial pressure; RV, right ventricular; RVEDP, RV end-diastolic pressure.

**p* < 0.05 versus Controls by Wilcoxon's test.

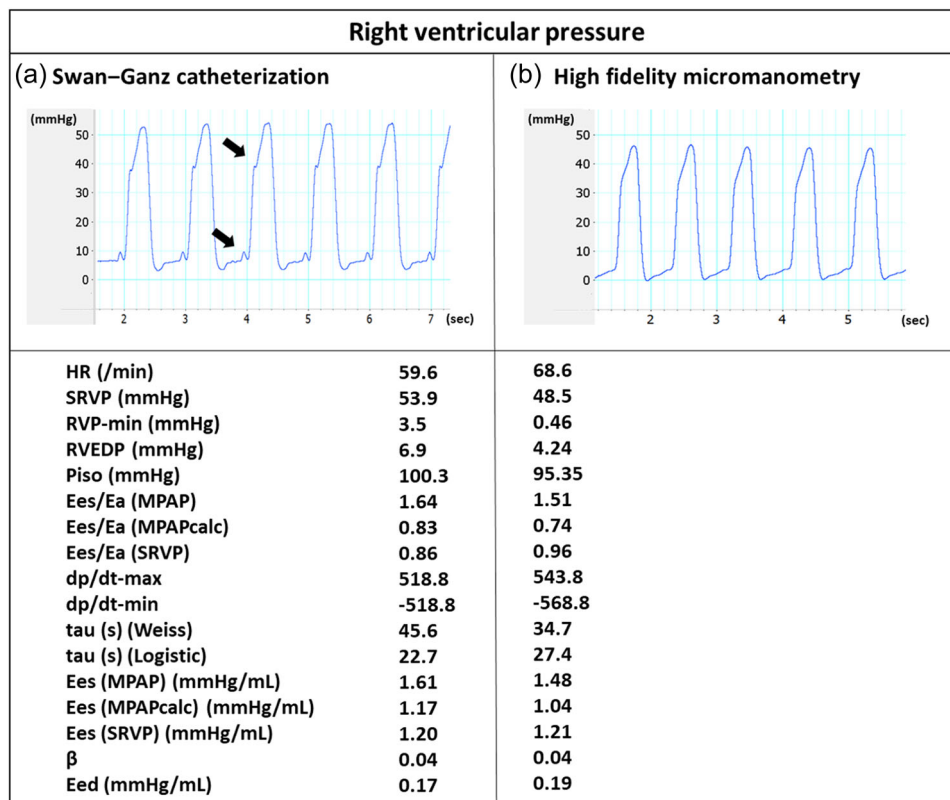


FIGURE 1 Representative image of right ventricular pressure recorded via Swan–Ganz catheterization and high-fidelity micromanometry. SG-cath-derived RVP showed fluctuations or notches near end-diastole and after the steep increase in the systolic phase (arrows) (a), whereas Pressure-cath-derived RVPs showed no or slight fluctuations/notches (b). In addition, SG-cath-derived RVP and calculated indices of RV function, including Ees (MPAP), Ees (MPAPcalc), Ees/Ea (MPAP), Ees/Ea (MPAPcalc), β , and Eed, were higher than those obtained by Pressure-cath. dp/dt-max, maximum dp/dt; dp/dt-min, minimum dp/dt; Ea, arterial elastance; Eed, end-diastolic elastance; Ees, end-systolic elastance; MPAP, mean pulmonary arterial pressure; MPAPcalc, calculated end-systolic pressure using MPAP; Piso, isovolumic pressure; Pressure-cath, high-fidelity micromanometry; RVEDP, right ventricular end-diastolic pressure; RVP, right ventricular pressure; SG-cath, Swan–Ganz catheterization; SRVP, systolic right ventricular pressure

confirmed or suspected PH. The results indicated that SG-cath-derived RV indices were similar to the corresponding Pressure-cath-derived indices, with neither significant differences nor obvious systematic trends as shown by Bland-Altman analysis findings. In addition, SG-cath-derived RV indices with proven prognostic value (Ees/Ea and β) exhibited good correlations ($ICC \geq 0.6$) compared with the corresponding Pressure-cath-derived indices.

Bachman et al.¹⁰ assessed RVP and calculated dp/dt-max and dp/dt-min via SG-cath and found significant correlations with the corresponding Pressure-cath-derived values in 13 participants suspected of having PH. Their study indicated a promising role of SG-cath-derived pressure analysis in the evaluation of RV function. However, Piso was not calculated in their study. Consequently, the suitability of using SG-cath data to calculate Ees and Ees/Ea was not examined. In addition, Bachman et al.¹⁰ calculated dp/dt-min but did

not calculate tau, β , and Eed. Thus, their study did not fully examine the accuracy of emerging SG-cath-derived indices of systolic and diastolic RV functions, as was performed in this study in a larger population.

Among the three RVP-derived indices that are associated with the systolic RV function (Ees, Ees/Ea, and dp/dt-max), Ees/Ea is considered to have the highest clinical value; moreover, it is significantly associated with the outcome of patients with PH.^{5,22,26,27} Notably, there are several variations in the calculation methods of Ees/Ea. For example, in previous reports (including ours)^{5,22,28} MPAP was used as Pes, and thus Ees/Ea was calculated using the formula $Piso/MPAP - 1$. Alternatively, Pes is approximately equal to SRVP in patients with severe PH; hence, using SRVP as Pes may be a reasonable option to calculate Ees/Ea.²⁶ Furthermore, a recent study reported that modified MPAP calculated using the formula $(1.65 \times MPAP - 7.79)$ is another surrogate candidate for Pes.¹⁷ With this background, in the present study,

TABLE 3 Comparison of right ventricular pressure and indices of right ventricular function evaluated with Swan–Ganz catheterization and high-fidelity micromanometry

| | Swan–Ganz catheterization | High-fidelity micromanometry | Bland–Altman plot, mean difference (limits of agreement) | Intraclass correlation coefficient |
|---|---------------------------|------------------------------|--|------------------------------------|
| Total subjects (n= 73) | | | | |
| HR (/min) | 69.8 ± 1.4 | 71.1 ± 1.4 | −1.3 (7.7, −10.3) | 0.92 |
| SRVP (mmHg) | 47.5 ± 2.1 | 43.0 ± 2.0 | 4.5 (11.3, −2.2) | 0.95 |
| RVP-min (mmHg) | 2.3 ± 0.3 | 0.8 ± 0.3 | 1.5 (5.8, −2.8) | 0.62 |
| RVEDP (mmHg) | 6.6 ± 0.4 | 4.4 ± 0.3 | 2.2 (7.2, −2.9) | 0.49 |
| Piso (mmHg) ^a | 67.9 ± 2.9 | 62.0 ± 2.1 | 6.0 (32.9, −21.0) | 0.77 |
| Ees/Ea (MPAP) ^b | 1.46 ± 0.08 | 1.28 ± 0.06 | 0.18 (1.20, −0.84) | 0.60 |
| Ees/Ea (MPAPcalc) ^c | 0.89 ± 0.69 | 0.76 ± 0.61 | 0.13 (0.99, −0.72) | 0.76 |
| Ees/Ea (SRVP) ^d | 0.48 ± 0.04 | 0.53 ± 0.04 | −0.05 (0.53, −0.62) | 0.65 |
| dp/dt-max (mmHg/s) | 502.6 ± 20.6 | 427.1 ± 13.7 | 75.5 (325.4, −174.4) | 0.57 |
| dp/dt-min (mmHg/s) | −467.5 ± 18.4 | −445.4 ± 18.0 | −22.1 (119.2, −163.3) | 0.89 |
| Tau (s) (Weiss) | 43.5 ± 2.4 | 44.0 ± 2.0 | −0.5 (25.0, −26.1) | 0.76 |
| Tau (s) (Logistic) | 27.8 ± 1.5 | 35.5 ± 1.7 | −7.7 (24.8, −40.2) | 0.22 |
| Subjects with CMRI study (n= 50) | | | | |
| Ees (MPAP) (mmHg/ml) ^e | 0.78 ± 0.06 | 0.63 ± 0.04 | 0.14 (0.74, −0.46) | 0.63 |
| Ees (MPAPcalc) (mmHg/ml) ^f | 0.55 ± 0.37 | 0.41 ± 0.30 | 0.14 (0.74, −0.46) | 0.54 |
| Ees (SRVP) (mmHg/ml) ^g | 0.34 ± 0.04 | 0.39 ± 0.05 | 0.06 (0.59, −0.48) | 0.65 |
| β^h | 0.027 ± 0.002 | 0.024 ± 0.001 | 0.002 (0.02, −0.013) | 0.71 |
| Eed (mmHg/ml) ⁱ | 0.16 ± 0.02 | 0.12 ± 0.01 | 0.04 (0.2, −0.12) | 0.57 |

Note: Data are shown as mean ± standard error (SE).

Abbreviations: CMRI, cardiac magnetic resonance imaging; dp/dt-max, maximum dp/dt; dp/dt-min, minimum dp/dt; Ea, arterial elastance; Eed, end-diastolic elastance; Ees, end-systolic elastance; HR, heart rate; MPAP, mean pulmonary arterial pressure; MPAPcalc, calculated end-systolic pressure using MPAP; Piso, isovolumic pressure; RVEDP, right ventricular end-diastolic pressure; RVEDV, right ventricular end-diastolic volume; RVP-min, minimum right ventricular pressure; RVS, right ventricular stroke volume; RVV, right ventricular volume; SRVP, systolic right ventricular pressure.

^aCalculated using the single-beat method.¹⁴

^bCalculated with the following formula: (Piso/MPAP) − 1.

^cCalculated with the following formula: (Piso/[1.65 × MPAP − 7.79]) − 1.

^dCalculated with the following formula: (Piso/SRVP) − 1.

^eCalculated with the following formula: (Piso − MPAP)/(CMRI-derived RVS).

^fCalculated with the following formula: (Piso − MPAPcalc)/(CMRI-derived RVS).

^gCalculated with the following formula: (Piso − SRVP)/(CMRI-derived RVS).

^hCalculated by solving the equations: $RVP = \alpha(eRVV \cdot \beta - 1)$ ($n = 48$).

ⁱCalculated using the following formula: $Eed = \alpha \cdot \beta \cdot eRVEDV \cdot \beta$ ($n = 48$).

we calculated Ees/Ea (MPAP), Ees/Ea (MPAPcalc), as well as Ees/Ea (SRVP), and demonstrated insignificant differences in both SG- and Pressure-cath-derived indices. In addition, the ICCs of SG- and Pressure-cath-derived data were good for all three Ees/Ea ratios: Ees/Ea (MPAP) (ICC = 0.60), Ees/Ea (MPAPcalc) (ICC = 0.76), and Ees/Ea (SRVP) (ICC = 0.65). This indicates that Ees/Ea can be used as an accurate parameter that reflects RV-PA coupling in patients with PH, particularly when MPAPcalc is used as Pes.

Ees/Ea can also be calculated using the “volume method” in which only volume data are used.²⁰ Brewis et al.²⁰ reported that volume-method-derived Ees/Ea (RVS/RVES) was an independent predictor of outcomes of patients with PA hypertension. However, volume-method-derived Ees/Ea is a mathematical transformation of RVEF [RVEF/(1 − RVEF)]. Further, it is considered to underestimate the true Ees/Ea, particularly in patients with PH. The clinical relevance of pressure- and volume-method-derived

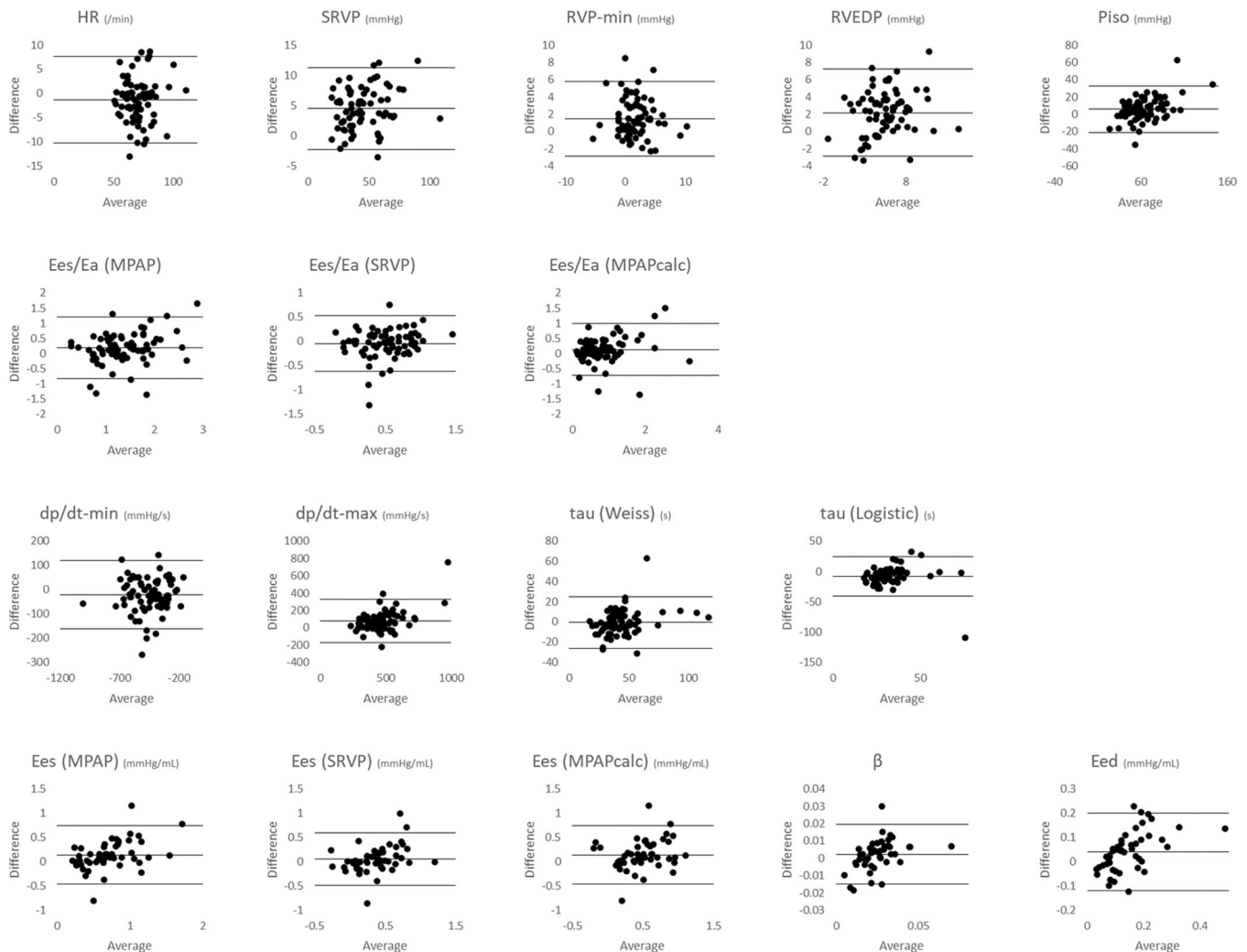


FIGURE 2 Bland–Altman plots of 13 SG- and Pressure-cath-derived indices of RVP. There were no systematic trends based on the values of the 13 indices. In all indices, the limits of agreement included 0, indicating that there were no significant differences between SG- and Pressure-cath-derived indices. dp/dt-max, maximum dp/dt; dp/dt-min, minimum dp/dt; Ea, arterial elastance; Eed, end-diastolic elastance; Ees, end-systolic elastance; HR, heart rate; MPAP, mean pulmonary arterial pressure; MPAPcalc, calculated end-systolic pressure using MPAP; Piso, isovolumic pressure; Pressure-cath, high-fidelity micromanometry; RV, right ventricular; RVEDP, RV end-diastolic pressure; RVP-min, minimum RV pressure; SG-cath, Swan–Ganz catheterization; SRVP, systolic RV pressure

Ees/Ea ratios requires further investigation in future clinical studies.

Indices of diastolic RV function derived from RVP analysis include dp/dt-min, tau, β , and Eed.²⁹ Among these, β and Eed reflect RV stiffness, and are associated with the outcomes of patients with PH.^{8,22} In the present study, SG-cath-derived β was comparable to Pressure-cath-derived β , whereas SG-cath-derived Eed tended to be higher than Pressure-cath-derived Eed, although the difference was not statistically significant. Meanwhile, SG-cath-derived β exhibited higher ICC (0.71) than SG-cath-derived Eed (0.57) when compared with the corresponding Pressure-cath-derived values. These indicate that β might be more suitable than Eed for the assessment of RV stiffness when SG-cath recordings are used.

The following reasons may explain the differences in RV indices between SG- and Pressure-cath-based evaluations. First, the effects of whipping and/or bending of a Swan–Ganz catheter may have caused the differences. Notably, as shown in Figure 1, the pressure waves obtained by SG-cath exhibited more fluctuations and notches than those of Pressure-cath recordings. Such artifacts might cause differences in RVP indices between SG- and Pressure-cath. Moreover, the artifacts can cause a recording of steeper incremental and decremental RVP changes, thereby increasing dp/dt-max and decreasing dp/dt-min. In addition, this could theoretically cause an overestimation of Piso, which would lead to overestimations of Ees and Ees/Ea. Second, the measurement of pressure using a water-filled catheter is known to have a

TABLE 4 Right ventricular pressure and indices of right ventricular function in controls and in patients with pulmonary hypertension

| Data from the entire subjects (n = 73) | | | | |
|--|--|--------------------------------------|---|--------------------------------------|
| n | Swan-Ganz catheterization-derived data | | High-fidelity micromanometry-derived data | |
| | Controls | Patients with pulmonary hypertension | Controls | Patients with pulmonary hypertension |
| | 16 | 57 | 16 | 57 |
| SRVP (mmHg) | 29.1 ± 5.0 | 52.7 ± 16.6* | 25.7 ± 5.0 | 47.8 ± 16.1** |
| RVP-min (mmHg) | 0.8 ± 2.6 | 2.7 ± 2.7* | 0.0 ± 2.2 | 1.0 ± 3.0 |
| RVEDP (mmHg) | 4.5 ± 3.0 | 7.2 ± 3.0* | 3.3 ± 2.0 | 4.8 ± 2.8** |
| Piso (mmHg) ^a | 47.6 ± 13.8 | 73.6 ± 23.9* | 44.1 ± 8.2 | 67.0 ± 17.1** |
| Ees/Ea (MPAP) ^b | 2.00 ± 0.86 | 1.31 ± 0.50* | 1.80 ± 0.47 | 1.13 ± 0.44** |
| Ees/Ea (MPAPcalc) ^c | 1.68 ± 0.90 | 0.67 ± 0.40* | 1.51 ± 0.69 | 0.55 ± 0.37** |
| Ees/Ea (SRVP) ^d | 0.64 ± 0.41 | 0.44 ± 0.36* | 0.73 ± 0.20 | 0.47 ± 0.34** |
| dp/dt-max (mmHg/s) | 396.4 ± 87.0 | 532.4 ± 183.6* | 329.3 ± 65.4 | 454.5 ± 113.4** |
| dp/dt-min (mmHg/s) | -292.9 ± 74.3 | -516.5 ± 138.9* | -280.5 ± 58.7 | -491.7 ± 139.3** |
| Tau (s) (Weiss) | 37.5 ± 19.2 | 45.2 ± 20.4 | 38.9 ± 11.0 | 45.4 ± 18.1 |
| Tau (s) (Logistic) | 27.7 ± 12.1 | 27.8 ± 12.8 | 37.6 ± 25.5 | 34.9 ± 9.7 |
| Data from the subjects who underwent CMRI (n = 50) | | | | |
| n | Swan-Ganz catheterization-derived data | | High-fidelity micromanometry-derived data | |
| | Controls | Patients with pulmonary hypertension | Controls | Patients with pulmonary hypertension |
| | 10 | 40 | 10 | 40 |
| Ees (MPAP) (mmHg/ml) ^e | 0.63 ± 0.22 | 0.81 ± 0.47 | 0.53 ± 0.09 | 0.66 ± 0.34 |
| Ees (MPAPcalc) (mmHg/ml) ^f | 0.58 ± 0.22 | 0.54 ± 0.40 | 0.48 ± 0.08 | 0.39 ± 0.33 |
| Ees (SRVP) (mmHg/ml) ^g | 0.38 ± 0.19 | 0.40 ± 0.40 | 0.34 ± 0.09 | 0.34 ± 0.31 |
| Ea (MPAP) (mmHg/ml) ^h | 0.29 ± 0.07 | 0.65 ± 0.37* | 0.29 ± 0.07 | 0.65 ± 0.37** |
| Ea (MPAPcalc) (mmHg/ml) ⁱ | 0.34 ± 0.11 | 0.92 ± 0.57* | 0.34 ± 0.11 | 0.92 ± 0.57** |
| Ea (SRVP) (mmHg/ml) ^j | 0.54 ± 0.10 | 1.06 ± 0.60* | 0.48 ± 0.08 | 0.97 ± 0.55** |
| β ^k | 0.020 ± 0.013 | 0.029 ± 0.013 | 0.021 ± 0.007 | 0.026 ± 0.010 |
| Eed (mmHg/ml) ^l | 0.13 ± 0.10 | 0.17 ± 0.11 | 0.11 ± 0.05 | 0.13 ± 0.08 |

Note: Data are shown as mean ± standard error (SE).

Abbreviations: CMRI, cardiac magnetic resonance imaging; dp/dt-max, maximum dp/dt; dp/dt-min, minimum dp/dt; Ea, arterial elastance; Eed, end-diastolic elastance; Ees, end-systolic elastance; HR, heart rate; MPAP, mean pulmonary arterial pressure; MPAPcalc, calculated end-systolic pressure using MPAP; Piso, isovolumic pressure; RVEDP, right ventricular end-diastolic pressure; RVEDV, right ventricular end-diastolic volume; RVP-min, minimum right ventricular pressure; RVSV, right ventricular stroke volume; RVV, right ventricular volume; SRVP, systolic right ventricular pressure.

^aCalculated using the single-beat method.¹⁴

^bCalculated with the following formula: (Piso/MPAP) - 1.

^cCalculated with the following formula: (Piso/[1.65 × MPAP - 7.79]) - 1

^dCalculated with the following formula: (Piso/SRVP) - 1.

^eCalculated with the following formula: (Piso - MPAP)/(CMRI-derived RVSV).

^fCalculated with the following formula: (Piso - [1.65 × MPAP - 7.79])/(CMRI-derived RVSV).

^gCalculated with the following formula: (Piso - SRVP)/(CMRI-derived RVSV).

^hCalculated with the following formula: MPAP/(CMRI-derived RVSV).

ⁱCalculated with the following formula: MPAPcalc/(CMRI-derived RVSV).

^jCalculated with the following formula: SRVP/(CMRI-derived RVSV).

^kCalculated by solving the equations: $RVP = \alpha (e^{RVV \cdot \beta} - 1)$ (n = 48 [controls, n = 10; patients with pulmonary hypertension, n = 38]).

^lCalculated using the following formula: $Eed = \alpha \cdot \beta \cdot e^{RVEDV \cdot \beta}$ (n = 48 [controls, n = 10; patients with pulmonary hypertension, n = 38]).

* < 0.05 versus Controls (Swan-Ganz catheterization-derived data) by Wilcoxon's test.

** 0.05 versus Controls (High-fidelity micromanometry-derived data) by Wilcoxon's test.

limited frequency response,⁹ which might cause inaccuracies. Finally, an arbitrary setting of the zero level in SG-cath might confound recordings. In our study, the pressure transducer was set to zero at the mid-thoracic line for SG-cath, as recommended.¹⁴ However, the obtained pressure could be directly affected by the zero leveling method. These suggest that a careful setup, including zero leveling, and efforts to diminish catheter flipping and bending during data acquisition are required to minimize possible inaccuracies when SG-cath is employed.

This study has some limitations. First, we used Pressure-cath for the validation of SG-cath-derived data, although the true gold standard method for calculating RV indices is multiple pressure-volume loop analysis (“multiple beat” method).¹¹ Pressure-cath provides more accurate pressure recordings than SG-cath and is less invasive than the multiple beat method. However, it should be noted that we used a simplified method (“single-beat” method) for calculating P_{es} and RV indices. Second, the SG- and Pressure-cath were not performed simultaneously. However, the two catheterizations were performed consecutively, mostly within 15 min, and participants were instructed to maintain a stable breath hold in the same manner for both catheterizations. Third, CMRI was not performed in 23 of the 73 participants; thus, E_{es} , β , and E_{ed} were calculated only in the remaining 50 participants. Fourth, different examiners performed SG- and Pressure-cath, which might have affected the results; nevertheless, the use of different examiners reduced the examination duration (within 15 min in most cases) and examination-related risks. Finally, the present study only aimed to validate the accuracy of SG-cath-derived indices of RV function. The relevance of using SG-cath-derived indices in clinical settings needs to be examined in future prospective studies on a sufficiently large number of patients.

In conclusion, this study examined the accuracy of SG-cath-derived indices of RV function in patients with suspected or confirmed PH, and showed that clinically relevant RV indices, such as E_{es}/E_{ea} and β , were similar and exhibited good correlations with the reference values obtained by Pressure-cath. It is expected that a suitable application of RV indices will promote a better understanding of the RV function, optimal management, and improve outcomes in patients with PH.

AUTHOR CONTRIBUTIONS

Hideki Shima and Toshitaka Nakaya generated the study concept, collected and analyzed data, and wrote the manuscript draft. Ichizo Tsujino co-generated the study concept and collected and analyzed data. Junichi

Nakamura and Hiroshi Ohira performed Swan–Ganz and pressure catheterizations and recorded right ventricular pressure. Hideki Shima, Ayako Sugimoto, Takahiro Sato, and Taku Watanabe interpreted the data and revised the manuscript. Masaru Suzuki and Masaru Kato collected data on respiratory and connective tissue disease and revised the manuscript. Isao Yokota reviewed the statistical analysis. Satoshi Konno and Ichizo Tsujino supervised the entire study, including manuscript writing.

ACKNOWLEDGMENTS

The authors thank Mamiko Inoue MT and Mr. Hajime Hatanaka for their assistance in data collection and analysis. The authors would like to thank Editage (www.editage.com) for English language editing.

CONFLICTS OF INTEREST

Dr. Ichizo Tsujino, Dr. Takahiro Sato, and Dr. Satoshi Konno belong to an endowed department (Division of Respiratory and Cardiovascular Innovative Research) supported by Nihon Shinyaku Co., Ltd.; Nippon Boehringer Ingelheim Co., Ltd.; and Mochida Pharmaceutical Co., Ltd. Dr. Isao Yokota reports having received funding from the Japan Society for the Promotion of Science KAKENHI and from the Health, Labour, and Welfare Policy Research Grants. Dr. Yokota also received speaker fees from Chugai Pharmaceutical Co., AstraZeneca Japan, Tobacco Pharmaceutical Division, and Nippon Shinyaku Co., outside the submitted work.

ETHICS STATEMENT

This study was approved by the Institutional Review Board of Hokkaido University Hospital for Clinical Research (No. 016-0461). Owing to the retrospective nature of the study, informed consent was obtained on an opt-out basis, via the website of Hokkaido University Hospital (<https://www.huhp.hokudai.ac.jp/>).

ORCID

Ichizo Tsujino  <http://orcid.org/0000-0002-0196-9572>

REFERENCES

1. Vonk Noordegraaf A, Chin KM, Haddad F, Hassoun PM, Hemnes AR, Hopkins SR, Kawut SM, Langleben D, Lumens J, Naeije R. Pathophysiology of the right ventricle and of the pulmonary circulation in pulmonary hypertension: an update. *Eur Respir J*. 2019;53(1):1801900. <https://doi.org/10.1183/13993003.01900-2018>
2. van de Veerdonk MC, Kind T, Marcus JT, Mauritz GJ, Heymans MW, Bogaard HJ, Boonstra A, Marques KM, Westerhof N, Vonk-Noordegraaf A. Progressive right ventricular dysfunction in patients with pulmonary arterial

- hypertension responding to therapy. *J Am Coll Cardiol*. 2011; 58(24):2511–9. <https://doi.org/10.1016/j.jacc.2011.06.068>
3. Frost A, Badesch D, Gibbs J, Gopalan D, Khanna D, Manes A, Oudiz R, Satoh T, Torres F, Torbicki A. Diagnosis of pulmonary hypertension. *Eur Respir J*. 2019;53(1):1801904. <https://doi.org/10.1183/13993003.01904-2018>
 4. Sanz J, Sánchez-Quintana D, Bossone E, Bogaard HJ, Naeije R. Anatomy, function, and dysfunction of the right ventricle: JACC state-of-the-art review. *J Am Coll Cardiol*. 2019;73(12):1463–82. <https://doi.org/10.1016/j.jacc.2018.12.076>
 5. Nakaya T, Ohira H, Sato T, Watanabe T, Nishimura M, Oyama-Manabe N, Kato M, Ito YM, Tsujino I. Right ventriculo-pulmonary arterial uncoupling and poor outcomes in pulmonary arterial hypertension. *Pulm Circ*. 2020;10(3):2045894020957223. <https://doi.org/10.1177/2045894020957223>
 6. Sanz J, García-Alvarez A, Fernández-Friera L, Nair A, Mirelis JG, Sawit ST, Pinney S, Fuster V. Right ventriculo-arterial coupling in pulmonary hypertension: a magnetic resonance study. *Heart*. 2012;98(3):238–43. <https://doi.org/10.1136/heartjnl-2011-300462>
 7. Rain S, Handoko ML, Trip P, Gan CT, Westerhof N, Stienen GJ, Paulus WJ, Ottenheijm CA, Marcus JT, Dorfmueller P, Guignabert C, Humbert M, Macdonald P, Dos Remedios C, Postmus PE, Saripalli C, Hidalgo CG, Granzier HL, Vonk-Noordegraaf A, van der Velden J, de Man FS. Right ventricular diastolic impairment in patients with pulmonary arterial hypertension. *Circulation*. 2013;128(18):2016–25. <https://doi.org/10.1161/CIRCULATIONAHA.113.001873>
 8. Trip P, Rain S, Handoko ML, van der Bruggen C, Bogaard HJ, Marcus JT, Boonstra A, Westerhof N, Vonk-Noordegraaf A, de Man FS. Clinical relevance of right ventricular diastolic stiffness in pulmonary hypertension. *Eur Respir J*. 2015;45(6):1603–12. <https://doi.org/10.1183/09031936.00156714>
 9. de Vecchi A, Clough RE, Gaddum NR, Rutten MC, Lamata P, Schaeffter T, Nordsletten DA, Smith NP. Catheter-induced errors in pressure measurements in vessels: an in-vitro and numerical study. *IEEE Trans Biomed Eng*. 2014;61(6):1844–50. <https://doi.org/10.1109/TBME.2014.2308594>
 10. Bachman TN, Bursic JJ, Simon MA, Champion HC. A novel acquisition technique to utilize Swan-Ganz catheter data as a surrogate for high-fidelity micromanometry within the right ventricle and pulmonary circuit. *Cardiovasc Eng Technol*. 2013;4(2):183–91. <https://doi.org/10.1007/s13239-013-0124-z>
 11. Hsu S, Houston BA, Tampakakis E, Bacher AC, Rhodes PS, Mathai SC, Damico RL, Kolb TM, Hummers LK, Shah AA, McMahan Z, Corona-Villalobos CP, Zimmerman SL, Wigley FM, Hassoun PM, Kass DA, Tedford RJ. Right ventricular functional reserve in pulmonary arterial hypertension. *Circulation*. 2016;133(24):2413–22.
 12. Galiè N, Humbert M, Vachiery JL, Gibbs S, Lang I, Torbicki A, Simonneau G, Peacock A, Vonk Noordegraaf A, Beghetti M, Ghofrani A, Gomez Sanchez MA, Hansmann G, Klepetko W, Lancellotti P, Matucci M, McDonagh T, Pierard LA, Trindade PT, Zompatori M, Hoeper M. 2015 ESC/ERS guidelines for the diagnosis and treatment of pulmonary hypertension: The Joint Task Force for the Diagnosis and Treatment of Pulmonary Hypertension of the European Society of Cardiology (ESC) and the European Respiratory Society (ERS): Endorsed by: Association for European Paediatric and Congenital Cardiology (AEPC), International Society for Heart and Lung Transplantation (ISHLT). *Eur Respir J*. 2015;46(4):903–75. <https://doi.org/10.1183/13993003.01032-2015>
 13. Scheinman M, Evans GT, Weiss A, Rapaport E. Relationship between pulmonary artery end-diastolic pressure and left ventricular filling pressure in patients in shock. *Circulation*. 1973;47(2):317–24. <https://doi.org/10.1161/01.cir.47.2.317>
 14. Rosenkranz S, Preston IR. Right heart catheterisation: best practice and pitfalls in pulmonary hypertension. *Eur Respir Rev*. 2015;24(138):642–52. <https://doi.org/10.1183/16000617.0062-2015>
 15. Clarke CJ, Gurka MJ, Norton PT, Kramer CM, Hoyer AW. Assessment of the accuracy and reproducibility of RV volume measurements by CMR in congenital heart disease. *JACC Cardiovasc Imaging*. 2012;5(1):28–37.
 16. Bellofiore A, Vanderpool R, Brewis MJ, Peacock AJ, Chesler NC. A novel single-beat approach to assess right ventricular systolic function. *J Appl Physiol*. 2018;124(2):283–90. <https://doi.org/10.1152/jappphysiol.00258.2017>
 17. Tello K, Richter MJ, Axmann J, Buhmann M, Seeger W, Naeije R, Ghofrani HA, Gall H. More on single-beat estimation of right ventriculoarterial coupling in pulmonary arterial hypertension. *Am J Respir Crit Care Med*. 2018;198(6):816–8.
 18. Weiss JL, Frederiksen JW, Weisfeldt ML. Hemodynamic determinants of the time-course of fall in canine left ventricular pressure. *J Clin Invest*. 1976;58(3):751–60. <https://doi.org/10.1172/JCI108522>
 19. Matsubara H, Takaki M, Yasuhara S, Araki J, Suga H. Logistic time constant of isovolumic relaxation pressure-time curve in the canine left ventricle. Better alternative to exponential time constant. *Circulation*. 1995;92(8):2318–26. <https://doi.org/10.1161/01.cir.92.8.2318>
 20. Brewis MJ, Bellofiore A, Vanderpool RR, Chesler NC, Johnson MK, Naeije R, Peacock AJ. Imaging right ventricular function to predict outcome in pulmonary arterial hypertension. *Int J Cardiol*. 2016;218:206–11. <https://doi.org/10.1016/j.ijcard.2016.05.015>
 21. Spruijt OA, de Man FS, Groepenhoff H, Oosterveer F, Westerhof N, Vonk-Noordegraaf A, Bogaard HJ. The effects of exercise on right ventricular contractility and right ventricular-arterial coupling in pulmonary hypertension. *Am J Respir Crit Care Med*. 2015;191(9):1050–7.
 22. Vanderpool RR, Pinsky MR, Naeije R, Deible C, Kosaraju V, Bunner C, Mathier MA, Lacomis J, Champion HC, Simon MA. RV-pulmonary arterial coupling predicts outcome in patients referred for pulmonary hypertension. *Heart*. 2015;101(1):37–43.
 23. Noordegraaf AV, Westerhof BE, Westerhof N. The relationship between the right ventricle and its load in pulmonary hypertension. *J Am Coll Cardiol*. 2017;69(2):236–43. <https://doi.org/10.1016/j.jacc.2016.10.047>
 24. Singh I, Oakland H, Elassal A, Heerdt PM. Defining end-systolic pressure for single-beat estimation of right ventricle-pulmonary artery coupling: simple... but not really. *ERJ Open Res*. 2021;7:3.
 25. Cicchetti F, Beach TG, Parent A. Chemical phenotype of calretinin interneurons in the human striatum. *Synapse*. 1998; 30(3):284–97. [https://doi.org/10.1002/\(SICI\)1098-2396\(199811\)30:3<284::AID-SYN6>3.0.CO;2-7](https://doi.org/10.1002/(SICI)1098-2396(199811)30:3<284::AID-SYN6>3.0.CO;2-7)

26. Richter MJ, Peters D, Ghofrani HA, Naeije R, Roller F, Sommer N, Gall H, Grimminger F, Seeger W, Tello K. Evaluation and prognostic relevance of right ventricular-arterial coupling in pulmonary hypertension. *Am J Respir Crit Care Med*. 2020;201(1):116–9.
27. Nakaya T, Tsujino I, Ohira H, Sato T, Watanabe T, Oyama-Manabe N, Nishimura M. Amelioration of right ventricular systolic function and stiffness in a patient with idiopathic pulmonary arterial hypertension treated with oral triple combination therapy. *Pulm Circ*. 2018;8(2):2045894018765350. <https://doi.org/10.1177/2045894018765350>
28. Trip P, Kind T, van de Veerdonk MC, Marcus JT, de Man FS, Westerhof N, Vonk-Noordegraaf A. Accurate assessment of load-independent right ventricular systolic function in patients with pulmonary hypertension. *J Heart Lung Transplant*. 2013;32(1):50–5. <https://doi.org/10.1016/j.healun.2012.09.022>
29. Murch SD, La Gerche A, Roberts TJ, Prior DL, MacIsaac AI, Burns AT. Abnormal right ventricular relaxation in pulmonary hypertension. *Pulm Circ*. 2015;5(2):370–5. <https://doi.org/10.1086/681268>

How to cite this article: Shima H, Nakaya T, Tsujino I, Nakamura J, Sugimoto A, Sato T, Watanabe T, Ohira H, Suzuki M, Kato M, Yokota I, Konno S. Accuracy of Swan–Ganz catheterization-based assessment of right ventricular function: validation study using high-fidelity micromanometry-derived values as reference. *Pulm Circ*. 2022;12:e12078. <https://doi.org/10.1002/pul2.12078>